Control Engineering Practice 19 (2011) 828–835

Contents lists available at ScienceDirect

Control Engineering Practice

journal homepage: www.elsevier.com/locate/conengprac

Fuzzy PDFF-IIR controller for PMSM drive systems

Stone Cheng*, Chi-Wei Li

Department of Mechanical Engineering, National Chiao Tung University, EE426, 1001 University Road, Hsinchu 300, Taiwan, ROC

ARTICLE INFO

Article history:
Received 3 February 2010
Accepted 8 April 2011
Available online 25 May 2011

Keywords:
PMSM
PDFF
Fuzzy control
Servo control
Field-oriented control

ABSTRACT

Pseudo-derivative feedback with feed-forward gain (PDFF) combines the advantages of proportional-integral (PI) and pseudo-derivative feedback (PDF) controllers. However, PDFF responds more slowly to a command than does PI. To increase the speed of response of the PDFF controller, this work presents a PDFF with moving average errors control. A low-pass IIR filter path for errors compensation that accelerates the slow response is added to a PDFF control loop. A fuzzy inferencer is utilized to adjust the feed-forward gain and integral gain of the PDFF controller to allow closed-loop poles of the transfer function to be properly placed to improve load torque disturbance rejection capability. Simulated and experimental results reveal that the response and load disturbance rejection ability of the fuzzy PDFF-IIR controller are better than those of the traditional PDFF controller.

1. Introduction

Permanent magnet synchronous motor (PMSM) servo drives are important in high-accuracy and high-performance drive systems in industrial motion control applications. In such applications, the classical multi-loop structure, in which each loop is controlled using an appropriate controller, has been extensively utilized. Currently, motor servo drivers in industrial products are based mostly on proportional-integral (PI) controllers. The PI controller has the advantages of a simple algorithm, high reliability, high stability, and excellent command response, but it tends to overshoot and provide a low DC stiffness. However, a favorable response and load disturbance rejection are very important in most motion control systems. The pseudo-derivative feedback with a feed-forward gain (PDFF) controller, which combines the advantages of PI and the pseudo-derivative feedback (PDF) controller, satisfies the aforementioned requirements. It provides a trade-off between the command response and the DC stiffness by appropriately tuning three constant gains. Furthermore, it avoids velocity overshoot when a motor accelerates or decelerates. Accordingly, the PDFF control algorithm provides a flexible solution in various cases of motion control.

Research on PDFF controllers has attracted attention in recent years. Some control design schemes for improving the performance of PDFF control or applications have been proposed, such as the papers by Liu and Li (2008), Cheng, Huang, and Chou (2008), and Tsai and Shen (2006, 2007). Furthermore, some robust PDFF controller products have been commercialized for industrial applications, including the VFD-VE series, introduced by Delta Electronics in 2007 and the Servostar CD series, introduced by Kollmorgen. Accordingly, the importance of PDFF control in servo systems has gradually increased. Self-tuning adaptive regulator controllers, that take both regulations and observations capabilities into account and are able to modify system parameters in order to maintain the desired response of the system, are being increasingly used (Li & Liu, 2009; Mohamed, 2007). However, the complexity of these algorithms is a large barricade to low cost PMSM drives.

The structure of PDFF controller is less responsive than PI algorithm under the same conditions, but allows closed-loop poles of the transfer function to be properly placed to improve load torque disturbance rejection capability (Romeral & Chekkouri, 2002; Shen & Tsai, 2006). In this study, a fuzzy PDFF-IIR controller with improved system response and load disturbance rejection capability is designed and analyzed. The fuzzy PDFF-IIR controller comprises three parts: (1) a PDFF scheme prevents overshoot; (2) a low-pass infinite impulse response (IIR) filter loop adjusts the system response, and (3) a fuzzy controller enhances the load disturbance rejection capacity. Each element of this combination is important and will be detailed. The important contributions of the proposed scheme are as follows:

- The structure of the fuzzy PDFF-IIR model provides dynamic feed-forward action a given drive constraints of stability margins. It also naturally adapts to varying environmental load disturbance conditions and can therefore be generalized to more complex applications. Furthermore, the PDFF and IIR model actions are kept simple for fuzzy inference algorithm to tune the parameters and therefore are easy to implement. The model requires only two gains to be adjusted by fuzzy inferencer over the entire operating range. The results of the

* Corresponding author. Fax: +886 35720634.
E-mail address: stonecheng@mail.nctu.edu.tw (S. Cheng).

0967-0661/$ - see front matter © 2011 Elsevier Ltd. All rights reserved.
doi:10.1016/j.conengprac.2011.04.011

experiment herein demonstrate that the fuzzy PDFF-IIR model is effective for controlling the PMSM system.

- The novelty of the proposed strategy is in the combination of PDFF, fuzzy inference, and an IIR filter scheme. The approach takes into account enhanced DC stiffness, the disturbance rejection, and the improvement in the response speed in a simple and highly efficient control law, as revealed by extensive experimental results.

2. Two-axis dynamic model of PMSM

Field-oriented control (FOC) is applied on the PMSM in the AC servo system. The field orientation of the PMSM requires that the dynamic equations in the stator axis frame be transformed to the rotor synchronous axis frame (d–q-axis). The nonlinear dynamic d–q model of the PMSM machine at the synchronous reference frame was derived in an adequate form (Chiasson, 2005). This model consists of nonlinear differential equations that relate the electrical quantities, currents, fluxes, and voltages, with the mechanical quantities, torque, and speed. The goal of the FOC is to perform real-time control of torque variations demand, control the rotor mechanical speed, and regulate phase currents in order to avoid current spikes during transient phases. To perform these controls, the electrical equations are projected from a 3 phase non-rotating frame into a 2-phase (d, q) system that rotates at the speed of the electrical speed of the rotor. In d–q coordinates, the PMSM electrical model equations are

$$\begin{cases} \begin{bmatrix} v_{ds} \\ v_{qs} \end{bmatrix} = \begin{bmatrix} R_s & -\omega_e L_{qs} \\ \omega_e L_{ds} & R_s \end{bmatrix} \begin{bmatrix} i_{ds} \\ i_{qs} \end{bmatrix} + \begin{bmatrix} L_{ds} & 0 \\ 0 & L_{qs} \end{bmatrix} \begin{bmatrix} \frac{d}{dt} i_{ds} \\ \frac{d}{dt} i_{qs} \end{bmatrix} + \begin{bmatrix} 0 \\ \omega_e \lambda_f \end{bmatrix} \\ T_e = \frac{3}{2}\frac{N_p}{2}\left[\lambda_f i_{qs} + (L_{ds} - L_{qs}) i_{ds} i_{qs}\right] \end{cases} \tag{1}$$

where v_{ds} and v_{qs} are the stator voltages of the d and the q axes, and i_{ds} and i_{qs} are the d and the q axes stator currents, respectively, R_s is the stator resistance, L_{ds} and L_{qs} denote the stator inductances of the d and the q axes, respectively; ω_e is the electrical angular velocity of the rotor, λ_f is the flux linkage of the rotor, T_e is the electromagnetic torque of the motor, and N_p is the number of poles of the motor. Therefore, the nonlinear state equations of i_{ds} and i_{qs} are given as

$$\begin{cases} \frac{di_{ds}}{dt} = \frac{1}{L_{ds}}(v_{ds} - R_s i_{ds} + \omega_e L_{qs} i_{qs}) \\ \frac{di_{qs}}{dt} = \frac{1}{L_{qs}}(v_{qs} - R_s i_{qs} - \omega_e L_{ds} i_{ds} - \omega_e \lambda_f) \end{cases} \tag{2}$$

It can be seen that the electromagnetic torque T_e can be controlled by regulation of currents i_{ds} and i_{qs} in closed loop. The direct-axis current i_{ds} corresponds to the component of stator magnetic field along the axis of the rotor magnetic field, while the quadrature-axis current i_{qs} corresponds to the orthogonal component. Considering field-oriented control for PMSM that i_{ds} does not contribute to the torque, voltage inputs are designed to guarantee the convergence of i_{ds} and i_{qs} to their desired control inputs i_{ds}^*, i_{qs}^*, by this means the control scheme yields $i_{ds}^* = 0$, the desired electromagnetic torque being directly proportional to the desired current input i_{qs}^*. For the currents, tracking control defines the current errors as

$$\begin{cases} e_{ds} = i_{ds}^* - i_{ds} \\ e_{qs} = i_{qs}^* - i_{qs} \end{cases} \tag{3}$$

And the dynamics derived from (2) and (3) are

$$\begin{cases} \frac{de_{ds}}{dt} = -\frac{1}{L_{ds}}(v_{ds} - R_s i_{ds} + \omega_e L_{qs} i_{qs}) \\ \frac{de_{qs}}{dt} = -\frac{1}{L_{qs}}(v_{qs} - R_s i_{qs} - \omega_e L_{ds} i_{ds} - \omega_e \lambda_f) \end{cases} \tag{4}$$

In order to ensure the convergence of the current errors to zero, the positive definite Lyapunov function is chosen as

$$V = \frac{1}{2}(e_{ds}^2 + e_{qs}^2) \tag{5}$$

The derivative of (5) is computed as

$$\begin{aligned} \dot{V} = e_{ds} \cdot \dot{e}_{ds} + e_{qs} \cdot \dot{e}_{qs} &= e_{ds}\left[-\frac{1}{L_{ds}}(v_{ds} - R_s i_{ds} + \omega_e L_{qs} i_{qs})\right] \\ &+ e_{qs}\left[-\frac{1}{L_{qs}}(v_{qs} - R_s i_{qs} - \omega_e L_{ds} i_{ds} - \omega_e \lambda_f)\right] \end{aligned} \tag{6}$$

To guarantee the global asymptotic stability in the current loop, the control voltage of d–q-axis is chosen as

$$\begin{cases} v_{ds} = K_{ds} L_{ds} e_{ds} + R_s i_{ds} - \omega_e L_{qs} i_{qs} \\ v_{qs} = K_{qs} L_{qs} e_{qs} + R_s i_{qs} + \omega_e (L_{ds} i_{ds} + \lambda_f) \end{cases} \tag{7}$$

where K_{ds} and K_{qs} are positive constant gains.

Substituting (7) into (6) the derivative of the Lyapunov function becomes

$$\dot{V} = -(K_{ds} e_{ds}^2 + K_{qs} e_{qs}^2) \le 0 \tag{8}$$

Clearly, (8) is only negative semi-definite. Since the PMSM must settle down at ($\dot{e}_{ds} = 0$, $\dot{e}_{qs} = 0$) and ($e_{ds} = 0$, $e_{qs} = 0$), according to the invariant set theorem (Haddad & Chellaboina, 2008), the system is globally asymptotically stable in the sense of Lyapunov at the origin. It implies that the resulting current closed-loop is asymptotically stable and, hence, the error variables e_{ds} and e_{qs} will converge to zero asymptotically.

However, the control of such drive system is complicated because of the coupling between all control inputs. This nonlinear dynamic model should be linearized to a linear time-invariant dynamic model for the PMSM machine at field orientation. On the other hand, the paper focuses on the motor–load system with low resonant frequency and small load–motor inertia ratio. The influence of the simplification of the two-mass system to the one-mass system on the dynamic property of the closed-loop control structure is small. In this case, the motor torque equation is

$$\begin{cases} \omega_e = \frac{N_p}{2}\omega_m \\ \underbrace{V_{qs}}_{\substack{q\text{-axis} \\ \text{voltage}}} = \underbrace{\overbrace{e_q G_{iq}}^{V_{qs}^* =}}_{\substack{q\text{-axis control} \\ \text{voltage}}} + \underbrace{\frac{N_p}{2}\omega_m \lambda_f}_{q\text{-axis back emf compensation}} \\ \underbrace{V_{ds}}_{\substack{d\text{-axis} \\ \text{voltage}}} = \underbrace{\overbrace{e_d G_{id}}^{V_{ds}^* =}}_{\substack{d\text{-axis control} \\ \text{voltage}}} - \frac{N_p}{2}\omega_m L_{qs} I_{qs} \\ I_{qs} = \frac{1}{(sL_{qs} + R_a)}\left(V_{qs} - \underbrace{\frac{N_p}{2}\omega_m \lambda_f}_{K_e}\right) \\ T_e = \frac{3N_p}{4}\lambda_f i_{qs} = K_T i_{qs} = J_m \frac{d\omega_m}{dt} + B_m \omega_m - T_L \end{cases} \tag{9}$$

where e_q is the error of q-axis current, G_{iq} is the controller of q-axis, s is the Laplace operator, K_T is the motor torque constant, T_L represents the torque disturbance, J_m is the moment of inertia, ω_m is the mechanical angular velocity of the rotor, and B_m is the viscous friction. Since the magnetic flux from the permanent magnetic rotor is fixed in relation to the rotor shaft position, the flux position in the d–q co-ordinates can be determined by the shaft-position sensor. Wallace, Novotny, Lorenz, and Divan (1994) noted that the increased torque per

ampere attainable is not severely affected by the effect of non-ideal field-oriented operation, indicating that this simple, constant parameter field-oriented controller can be applied in some situations without resorting to complex controllers, which compensate for the large flux changes.

3. Design and simulation of control system

3.1. Control scheme

Fig. 1 shows the function block diagram of speed controller and PMSM that adopts the FOC algorithm. The figure presents the fuzzy PDFF-IIR control scheme. Notably, the output of the low-pass IIR is added to the second summing point to enhance the system response. FLC is a fuzzy logic controller that is utilized to adjust the feed-forward gain (K_{ff}) and the integral gain (K_i) of the PDFF controller, to reduce the disturbance T_L.

The linear mathematical model of a PMSM plant transfer function from voltage command ω_r to motor speed ω_m can be modeled by a second-order system as

$$G_p(s)=\frac{K_t}{(sL_{ss}+R_a)(sJ_m+B_m)}=\frac{K_1}{(s+1/\tau_e)(s+1/\tau_m)} \tag{10}$$

where τ_m is mechanical time constant, and τ_e is electrical time constant of the PMSM plant. When high gain closed-loop current control is implemented as a minor-loop control, two poles are pushed apart, so that the mechanical time constant is increased, while the electrical time constant is decreased (7). With high gain current-loop control, the plant can be simplified as a first-order model of

$$G_p(s)=\frac{K_1\tau_e}{s+1/\tau_m} \tag{11}$$

For this system, a PDFF control structure (3) can be constructed by pole- placement type controller, because this scheme moves the locations of open-loop poles without affecting open-loop zeros, with a feed-forward term adding to the controller, as shown in Fig. 1. In order to study characteristics of the PDFF controllers, a set of transfer functions is derived by selecting various input and output points from Fig. 1 as shown in the following:

$$\begin{cases}\text{command to output}: G_c(s)=\frac{\omega_m(s)}{\omega_r(s)}=\frac{K_1\tau_e(K_i+sK_{ff})}{s^2+(1/\tau_m+K_1\tau_eK_f)s+K_1\tau_eK_i}\\ \text{command to error}: G_e(s)=\frac{e(s)}{\omega_r(s)}=\frac{s^2+(1/\tau_m+K_1\tau_eK_f-K_1\tau_eK_{ff})s}{s^2+(1/\tau_m+K_1\tau_eK_f)s+K_1\tau_eK_i}\end{cases} \tag{12}$$

Consider steady-state error of unit step and ramp inputs, steady-state errors e_{ss} can be calculated by applying the final value theorem to (12) as

$$\begin{cases}\text{Unit step input}: e_{ss}=\lim\limits_{s\to0}\left(s\frac{G_e(x)}{s}\right)=0\\ \text{Ramp input}: \times e_{ss}=\frac{e(s)}{\omega_r(s)}=\lim\limits_{s\to0}\left(s\frac{G_e(s)}{s^2}\right)=\frac{1/\tau_m+K_1\tau_e(K_f-K_{ff})}{K_1\tau_eK_i}\end{cases} \tag{13}$$

Since the mechanical time constant of PMSM is large in most motion control applications, the ramp command error will be very small when the feed-forward gain and feedback gain are equal. A feed-forward gain K_{ff} injects the command ahead of the integral making the system more responsive to commands. When the application requires low-frequency stiffness, low K_{ff} gain allows much higher integral gain without inducing overshoot. Unfortunately, it also makes the system slower in responding to the command. The experiments of motion control with K_{ff}=60% usually give good results. Over the entire range of K_{ff} , the response increases in a velocity loop controller by about 45% and the DC stiffness declines by about five times. PDFF controller gives flexibility in performance requirements by tuning feed-forward gain and integral gain for best reference tracking response without overshoot, or greatest low-frequency stiffness.

Furthermore, to avoid oscillatory response in $G_c(s)$, the damping ratio must be $\zeta\geq0.707$, which gives the relationship between parameters of the PDFF controller

$$\begin{cases}1.5\geq\zeta=\frac{(1/\tau_m+K_1\tau_eK_f)}{2\sqrt{K_1\tau_eK_i}}\geq0.707\\ K_i\leq\frac{(1/\tau_m+K_1\tau_eK_f)^2}{2K_1\tau_e}\\ K_f\geq\frac{1.414\sqrt{K_1\tau_eK_i}-1/\tau_m}{K_1\tau_e}\end{cases} \tag{14}$$

3.2. Low-pass IIR path design

The low-pass IIR path and fuzzy logic controller are designed herein. First, the following two filters structures are considered. Experiments on system at sampling frequency of 5KHz is carried out to implement the IIR filter.

Filter 1:

$$IIR_1=F_1(z)=\frac{k}{c-bz^{-1}} \tag{15}$$

Eq. (15) is the transfer function of the first-order IIR, where k, b, and c are three positive tunable parameters. The values of these parameters affect the system response. A larger k corresponds to a

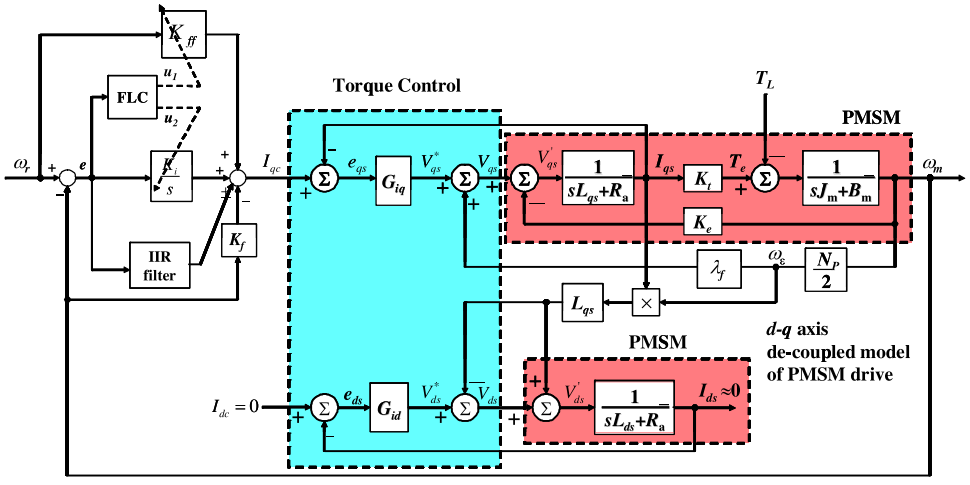

Fig. 1. Fuzzy PDFF-IIR velocity control scheme.

faster system response, because k is equivalent to the gain of IIR_1. Parameters c and b determine the pole of IIR_1. When the stable pole is closer to the unit circle in the z plane, the system response is fast. Fig. 2 compares the simulation results for velocity control loops associated with a PDFF controller with those associated with a PDFF plus IIR_1 path controller. The system response is improved by adding the low-pass IIR path to the traditional PDFF construction. However, a positive output from the IIR filter degrades system response. Additionally, PDFF with only IIR filter cannot reduce the step disturbance, because all areas under the velocity responsive curve are the same. For most motion systems, the area under the velocity response is commonly more important than the peak excursion, because the area under the velocity curve represents the error in the position of the system. Fig. 3(a) and (b) shows the effects of parameter k and the pole location of IIR_1, respectively, on the system response. In Fig. 3(a), the pole was set to 2/7 and remained constant. In Fig. 3(b), parameter k was set to unity and remained constant.

Filter 2:

Filter 1 is a simple low-pass IIR filter. Generally, the IIR filter design relies on a common analog filter to yield a digital filter. In Filter 2, a Butterworth low-pass filter $F_B(z)$ is applied to strengthen the system response. The order N and cutoff frequency ω_c of the filter are parameters that must be designed. Fig. 4(a) compares the results of the simulation of the velocity control loops with PDFF and those with PDFF plus a Butterworth IIR controller. Here, the IIR filter's cutoff frequency is 1 kHz and the order is two to compensate the velocity loop response of 500 Hz bandwidth. The figure shows that a negative output from the IIR filter can accelerate the system response but includes an overshoot. Hence, the design must be revised to reduce the output signal of the filter. The revised design satisfies

$$F'_B(z) = KF_B(z) \tag{16}$$

where $F_B(z)$ is the original Butterworth filter, $F'_B(z)$ is the modified Butterworth filter, and K is a constant gain between zero and unity that limits the filter's output. Fig. 4(b) compares the results of the simulation of the velocity control loops with PDFF with those of PDFF plus the modified Butterworth IIR controller with $K=0.45$.

Fig. 5 presents the influence of the order N and cutoff frequency on the system response. In Fig. 5(a), the cutoff frequency is set to 200 Hz, 1 kHz, and 3 kHz, and the order is two. The K gain is set to prevent overshoot. Intuitively, increasing the cutoff frequency considerably increases the system response. In Fig. 5(b), the cutoff frequency and K gain are set to 1 kHz and 0.4, respectively. A high-order Butterworth filter does not enhance the system response or make it smooth. A high-order filter produces vibration in the response. Consequently, the design should incorporate a lower-order Butterworth filter. In summary of the comparison of filters 1 and 2, IIR_1 has a simple structure and is easier to be

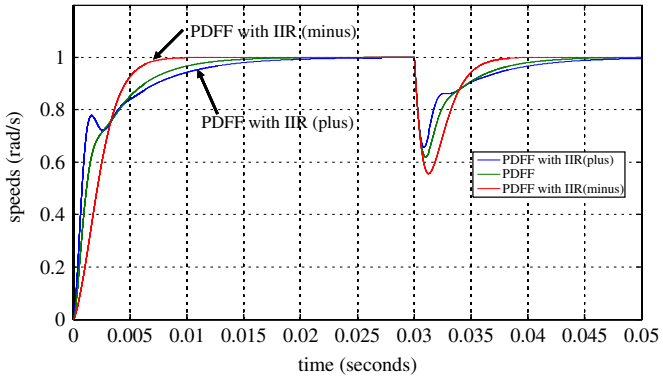

Fig. 2. Comparison of performance of PDFF and PDFF with IIR_1 controller.

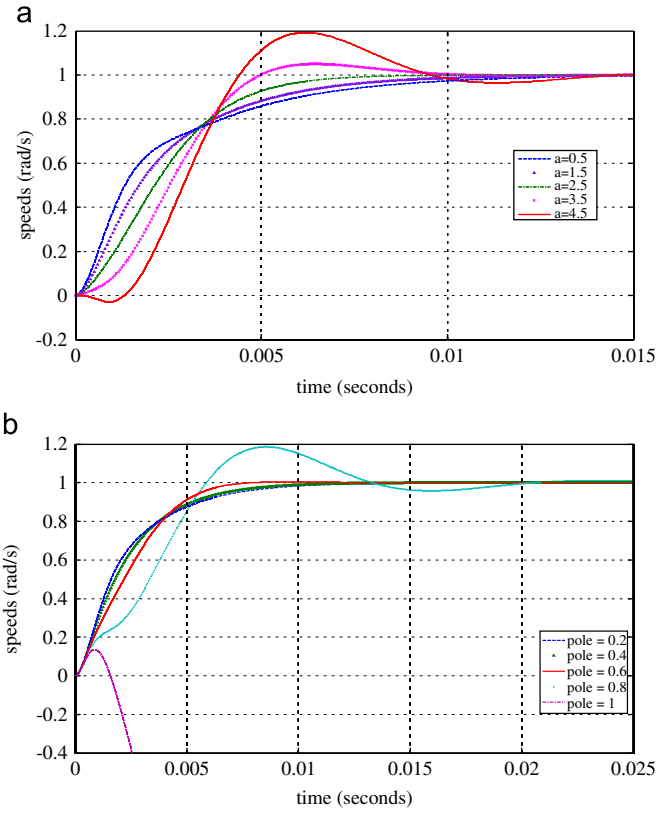

Fig. 3. System responses with varying parameters: (a) k and (b) pole locations.

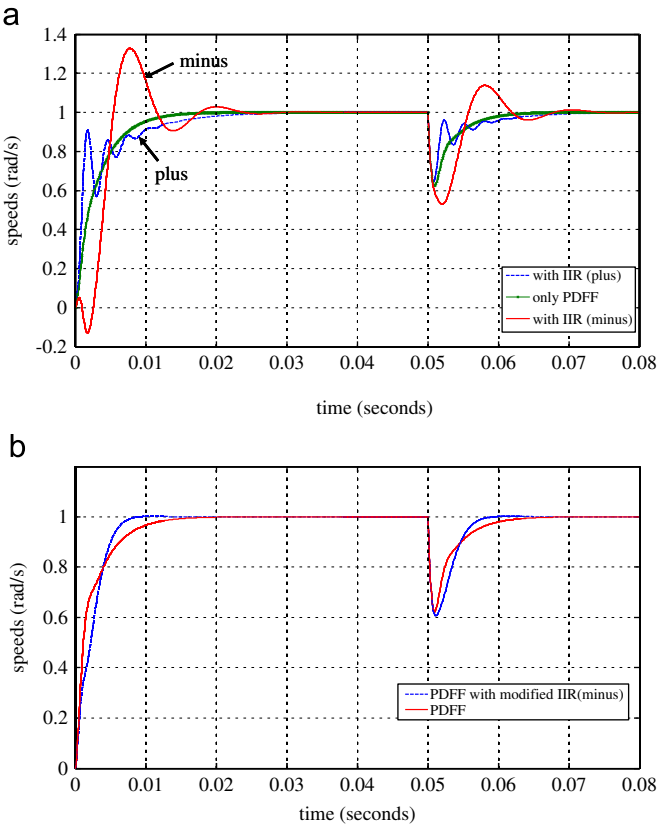

Fig. 4. Performance comparisons under the PDFF with Butterworth filter compensation: (a) original Butterworth filter and (b) modified Butterworth filter.

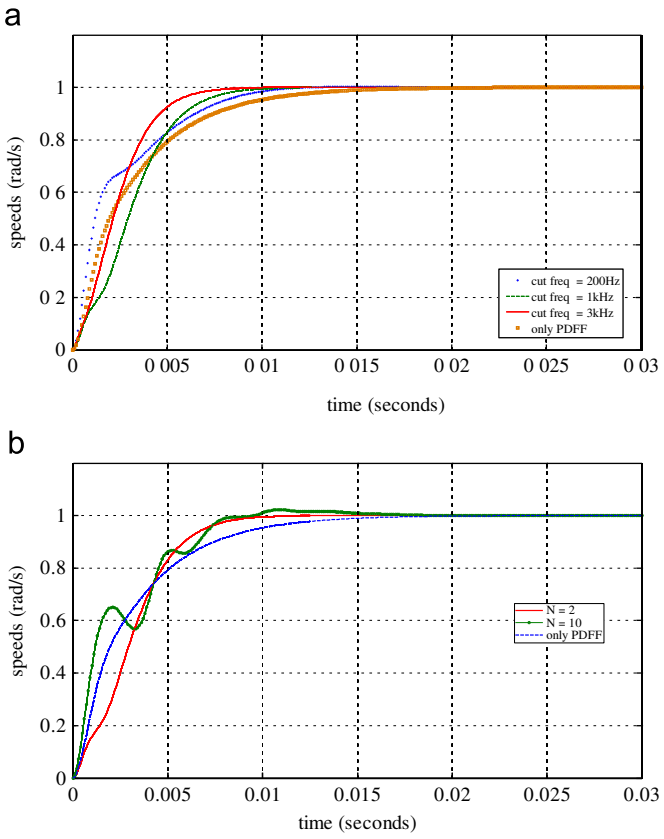

Fig. 5. Variation of system responses with (a) cutoff frequency and (b) order of the filter.

implemented than second-order filter. The determination of the parameters in both the filters is similar, with cutoff frequency and gain. Both methods improve the system response but neither reduces the load disturbance rejection. For this reason K_i and K_f should be set as high as possible.

3.3. Design of fuzzy logic controller

The above simulation results reveal that a controller using PDFF plus IIR improves only the system response and does not attenuate the step load disturbance. In this study, a fuzzy logic controller that exploits the properties of PDFF is designed to address load disturbance. Since PDFF combines the advantages of PI and PDF controllers, it frequently has a feed-forward gain (K_{ff}) to feedback gain (K_f) ratio of p. When p is one, PDFF and PI are equivalent; when p is zero, PDFF and PDF are equivalent. PDF is a simple one-degree-of-freedom controller and is less responsive to the reference input than is PI control, but it can provide a higher DC stiffness. Its contribution to the robustness of the system parameters and external disturbance rejection exceeds that of PI control, because DC stiffness is proportional to the integral gain (Ellis, 1999). However, PI control easily causes a large overshoot when the integral is high. In PDF control (Ellis & Lorenz, 1999; Ohm, 1994; Perdikaris, 1999), the entire signal is filtered by determining the integral. Therefore, the integral gain can be increased without causing overshoot, unlike in PI control.

In order to develop the supervisory system to tune the PDFF controller, some expressions must be carried out

- Eq. (13) shows that integral term K_i cannot lead to eliminate the ramp tracking error. It can be only reduced if K_i increases greatly.
- A feed-forward gain K_{ff} makes the system more responsive to commands.
- The effect of disturbance to the output is dependent on damping ratio, a normal choice of damping ratio would be 0.707–1.5.
- Pole-zero cancellation tuning should be avoided because of its poor robustness characteristics and slow load torque disturbance response.

In this investigation, the fuzzy tracking block uses the same Mamdani fuzzy reasoning method and centroid defuzzification approach. The fuzzy logic controller has a single normalized input variable (error signal, E) to simplify the design of the membership functions and two output variables (u_1 and u_2), where u_1 and u_2 are adopted to regulate the feed-forward gain and the integral gain, respectively. Here, one input variable suffices for the application of FLC to electrical system; the use of plant evolution variables, the derivative of the speed error, does not improve controller performance from the results of simulation and experiment. The fuzzy PDFF-IIR control algorithm is expressed as

$$i_{qc}(k) = \left(\frac{u_2 K_i}{1-z^{-1}}\right) e(k) + u_1 K_{ff} \omega_m^*(k) - K_{ff} \omega_m(k) + f_o(k) \tag{17}$$

where $e(k) = \omega_m^* - \omega_m/\omega_m^*$ is the normalized input, ω_m^* refers to the velocity set point at the kth sample time, and ω_m denotes the process output at the kth sample time. $f_o(k)$ is the IIR output signal.

The membership functions of the input and output variables that correspond to each fuzzy set are denoted as [NL, NM, NS, ZO, PS, PM, PL] and [Min, S, M, L, MAX], respectively. The member functions that describe the fuzzy input variable E and output variables u_1 and u_2 have the same isosceles triangular shape across the universe of discourse, as shown in Fig. 6. The universes of discourse of the input and output variable are each normalized to $[-1, 1]$, $[0, 1]$, and $[1, 5]$. The PDFF controller can be regarded as a generalized PI controller. The ratio of K_{ff}/K_f , with a range between 0 and 1, determines that the PDFF controller is approaching PI or PDF characteristics. Since K_f is set to one, the universe of discourse of u_1 is set to $[0, 1]$ to limit the ratio of the feed-forward gain (K_{ff}) to the feedback gain (K_f) in between zero and one. Furthermore, the effect of disturbance rejection capability to the output is dependent upon the ratio of K_i/K_f . The peak magnitude of the disturbance response can be reduced by increasing the K_i/K_f ratio. But as the ratio is increased, a reduced peak magnitude can only be achieved with the cost of slow settling time. A compromise must be made between optimizing peak magnitude and settling.

The main concept that underlies design of the fuzzy rule-based design is that PDFF should exhibit the characteristics of PI control to reach the set point rapidly when the error is large (Pajchrowski & Zawirski, 2008; Romeral & Chekkouri, 2002). Therefore, the feed-forward gain of the PDFF controller must be set high, and the integral gain must be set small, to prevent overshoot in this case. However, PDFF control exhibits the characteristics of PDF control when the error is small, in which case, overshooting is unlikely.

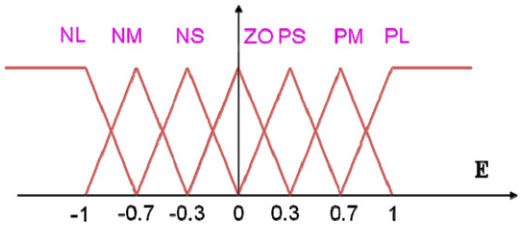

Fig. 6. Shape of input membership function.

Table 1
Fuzzy rule base.

E	NL	NM	NS	ZO	PS	PM	PL
u_1	Max	L	M	Min	M	L	Max
u_2	Min	S	M	Max	M	S	Min

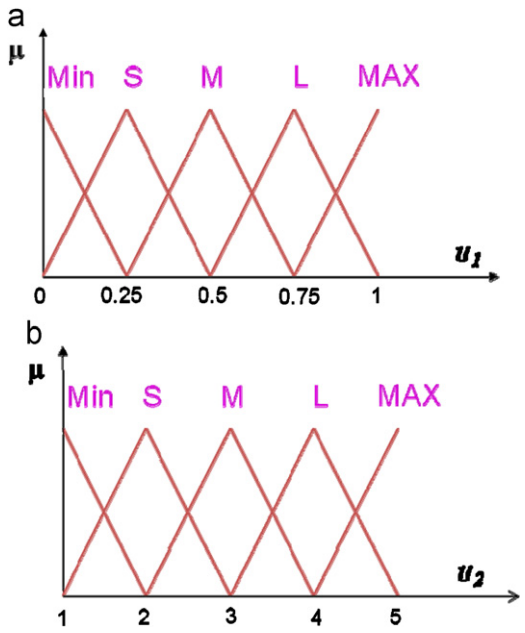

Fig. 7. Shape of output membership function: (a) u_1 and (b) u_2.

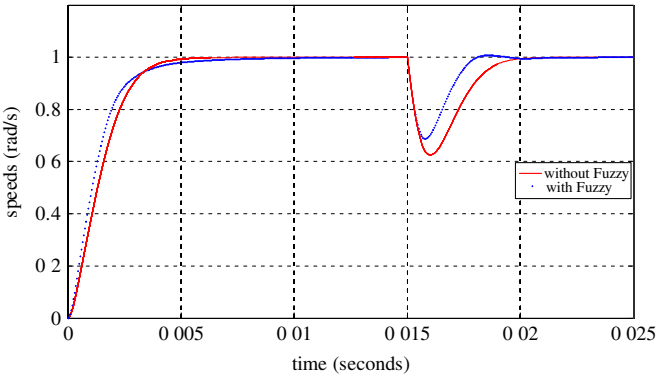

Fig. 8. Comparison of performance of PDFF-IIR and fuzzy PDF-IIR controller.

Simultaneously, the integral gain can be set high to increase the load disturbance rejection capacity. Table 1 presents the seven-term fuzzy rule table. A fuzzy rule has the form

If E is A_k, then (u_1 is B_k and u_2 is C_k), $k = 1,2,\ldots,N$

where E, u_1, and u_2 are the fuzzy input and output variables, as presented in Fig. 7; A_k, B_k, and C_k are fuzzy sets. Fig. 8 compares the original PDFF with IIR with fuzzy PDFF-IIR controllers. Here, the integral gain, feed-forward gain, and feedback gain of the two controllers are set to the same values. The IIR filter is a second-order Butterworth filter with a cutoff frequency of 1 kHZ. The ratio of the feed-forward gain to the feedback gain is 60%, which is commonly used in industrial control. Fig. 8 presents that the rise time of the fuzzy PDFF-IIR is faster than that of PDFF-IIR. Additionally, the load disturbance rejection capacity of fuzzy PDFF-IIR is better than that of PDFF-IIR control. However, the settling time is too long, and this problem becomes the main issue with fuzzy PDFF-IIR control. Fuzzy PDFF-IIR is similar to PDF control when the error is small, because the integrator dominates PDF control, but the integrator requires some time to accumulate error data to achieve control, which is expected to increase the delays in systems.

4. Experiments on PMSM drive system

Experiments on system at sampling frequency of 20KHz have been carried out to check the effectiveness of the proposed controller. The system consists of three main parts: (i) a PMSM coupled to a load through a torque detector, (ii) the current-regulated PWM motor drive, and (iii) a TMS320C2407 DSP implements the fuzzy PDFF-IIR digital control part for speed controller and current regulator. The measured data stored in the on-board dual port memory is then passed back to the PC host for performance evaluation. Fig. 9 shows the flowchart of the fuzzy PDFF-IIR control algorithms in DSP program for PMSM drive. The three control loops use the same interrupt clock to generate the different sampling rate for each loop. PMSMs with powers of 300 W and 1 kW are tested here. Table 2 shows the parameters of the PMSMs used in the experiment. PDFF-IIR controller conditions during fuzzy tuning procedure are nominal values as shown in Fig. 10.

Experiment 1 adopts a 1 kW PMSM; the reference velocity input is a 0.5 Hz square wave; the peak-to-peak voltage of velocity command is 2 V, which corresponds to 400 RPM motor speed, and the offset voltage is 1 V. The PI control algorithm is executed in the current loop and PDFF is used in the velocity loop of the drive system. Fig. 10 also describes a detailed data of IIR path to compensate for PDFF. To improve the load disturbance rejection capability, the parameters of PDFF are tuned to be close to those of PDF control: K_{ff}/K_f is set to 20%. Fig. 11 presents the step response of a 1 kW PMSM and drive system with IIR filter compensation in the velocity loop. It can be seen that the closed-loop system has a better speed response after the IIR filter compensation is added. Compared with the speed response without IIR tuning (60.2 ms settling time), the speed response under IIR tuning has a shorter settling time (45.8 ms). The IIR filter compensation can increase the bandwidth of the system. The peak current feedback is reduced to prevent the flow of the highest current. Fig. 12 plots the velocity step response in experiment 2, in which the 300 W PMSM was used in torque mode. In Fig. 12(a), PI control is applied in the current and velocity loops. PI used in the servo system easily causes overshoot. In Fig. 12(b), PI control is used in the current loop, and PDFF without IIR compensation is used in the velocity loop. If PDFF replaces PI, then the overshoot declined to one below that in Fig. 12(a). Fig. 12(c) reveals that IIR compensation can accelerate the system response. The experimental results indicate that the PDFF with IIR filter compensation demonstrates its superiority in both tracking and regulation conditions. It does not cause overshoot and its bandwidth is not lower than PI, the behavior of the system results is mostly improved.

5. Conclusions

This work developed a fuzzy PDFF-IIR control scheme for improving the response of traditional PDFF controllers. IIR filter compensation is added to the traditional PDFF controller,

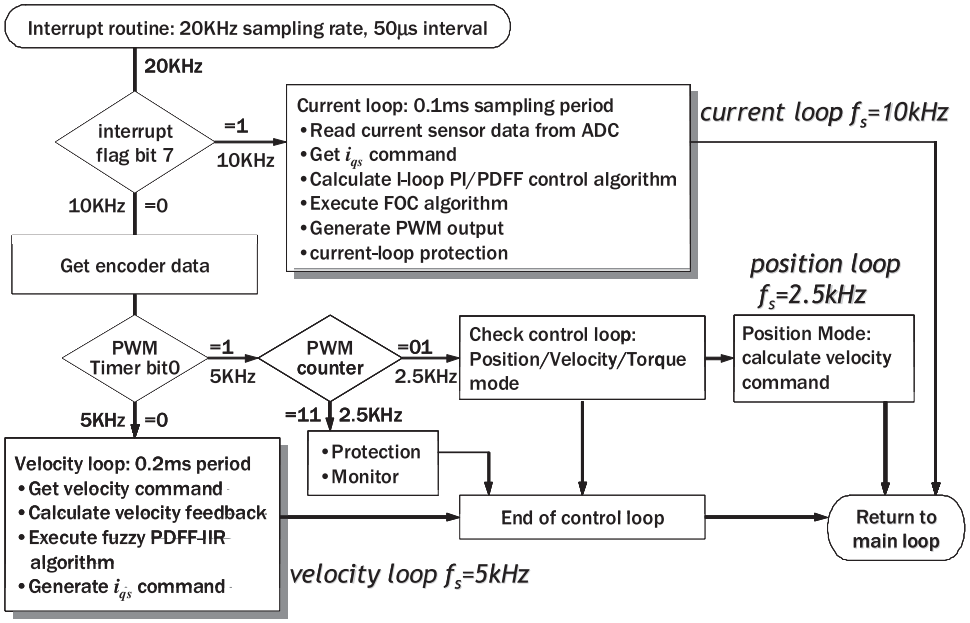

Fig. 9. Program flowchart of FOC and PDFF-IIR control scheme. Each loop has 50 μs execution time.

Table 2
Parameter values of PMSM used in experiment.

Rated power	300 W	1 kW
Moment inertia J_m (kg cm^2)	0.658	6.37
Armature resistance R_s (Ω)	8.37	1.82
Inductance L_{ds} and L_{qs} (mH)	17.4	10.05
Number of pole N_P	8	8
K_e (V/KRPM)	54.9	106.8
K_T (N m/A)	0.524	1.02
Rated voltage (V)	107.7	185.3
Rated speed (RPM)	3000	2000
Rated current (A)	2.0	5.16
Rated torque (N m)	0.95	4.782
Mechanical time constant (ms)	1.96	1.11
Electrical time constant (ms)	2.05	5.52

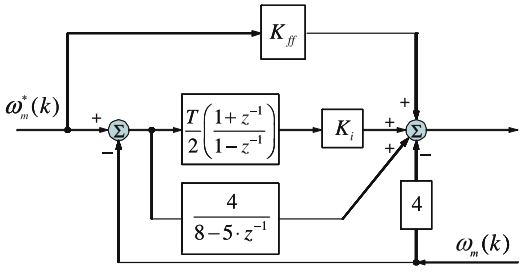

Fig. 10. PDFF-IIR control scheme with nominal values for experiment, where T=0.2 ms sampling period.

increasing its responsiveness to velocity commands. Next, a fuzzy inferencer is applied to compute the feed-forward gain and integral gain of the PDFF controller using a fuzzy rule base design procedure. The proposed control strategy was applied to PMSM drive systems, which was designed without either recursive estimations or model reference, but defining a self-tuning procedure by means of fuzzy logic. Typical simulation results and the experiments of loaded PMSM drive machinery show the favorable performance of the controlled system. To demonstrate the versatility of the proposed approach, two power motors were tested. A performance comparison with standard PDFF controller has

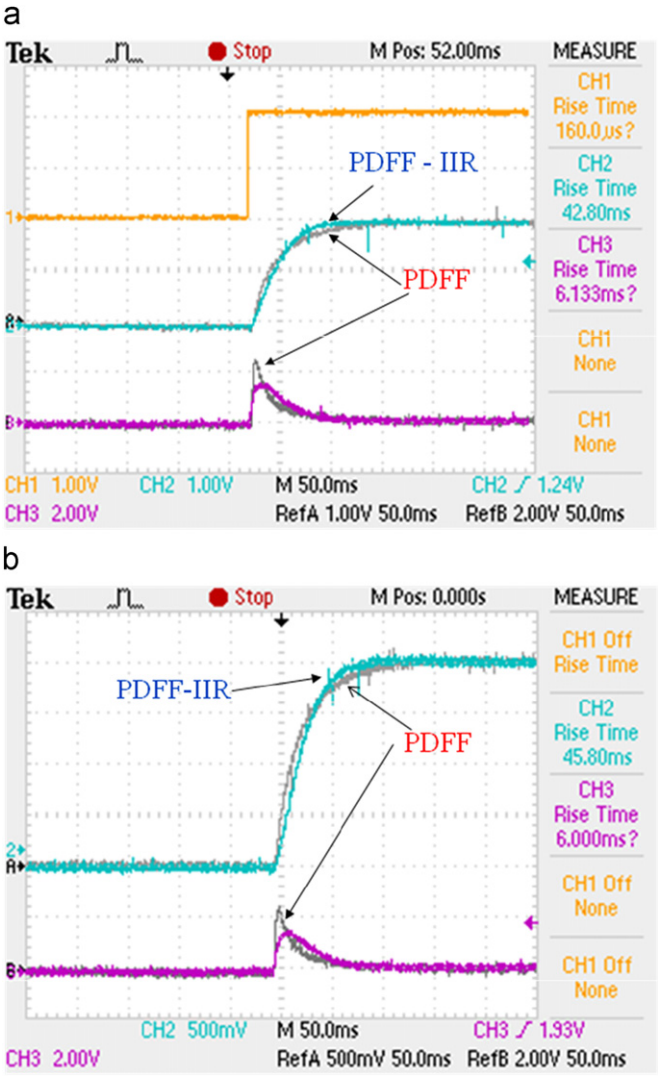

Fig. 11. 1 kW PMSM step response: (a) original and (b) magnified.

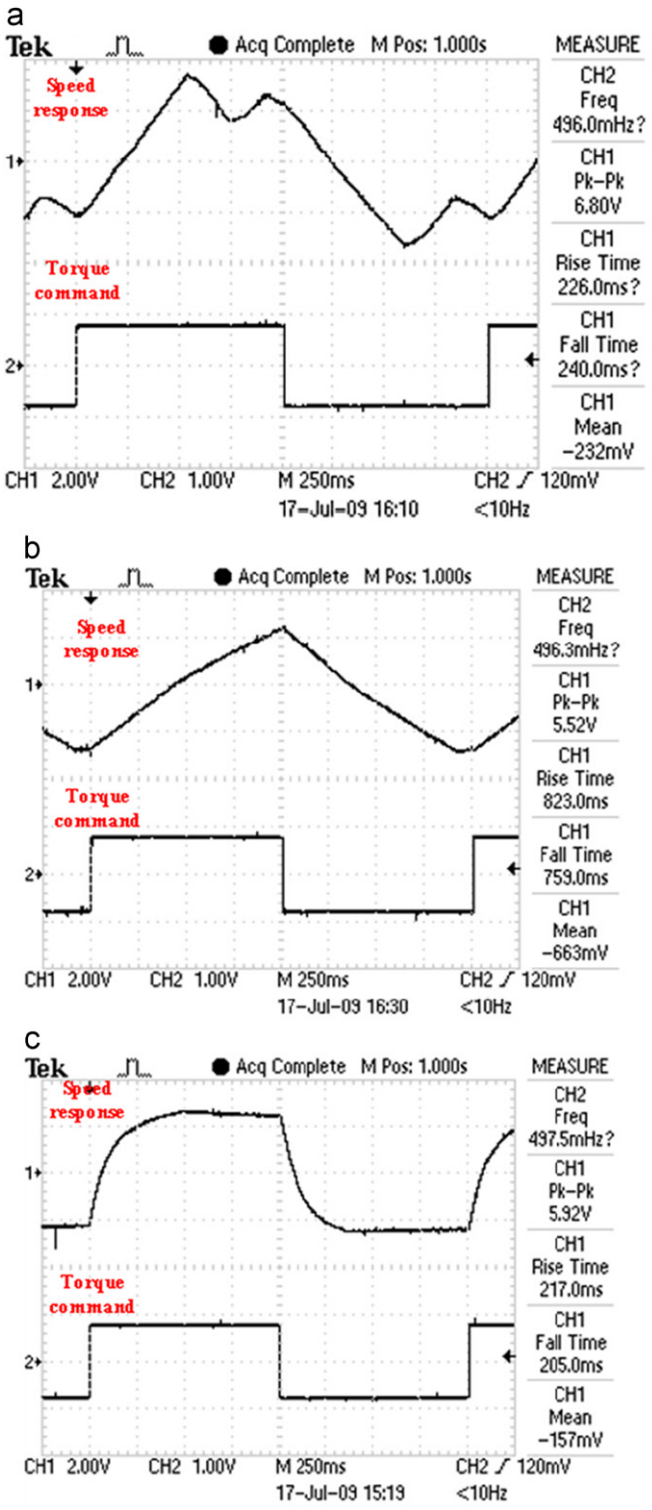

Fig. 12. 300 W PMSM step response with different controllers: (a) PI, (b) PDFF and (c) PDFF with IIR.

been made, confirming the superiority of the fuzzy PDFF-IIR controller. Additional advantage of the proposed controller is that it can be implemented easily to the existing digital signal processor that carries out the supervision without major revision of software structure.

References

Cheng, S., Huang, Y. Y., & Chou, H. H. (2008). Dual robust controller design for high power AC servo drive. In *Proceedings of the ECSIS symposium on learning and adaptive behaviors for robotic systems* (pp. 97–102). Edinburg, Scotland.

Chiasson, J. (2005). *Modeling and high-performance control of electric machines*. In IEEE Press series on power engineering. New Jersey: John Wiley & Sons, Inc.

Ellis, G. (1999). PDFF: An evaluation of a velocity loop control method. In *Proceedings of the PCIM-Europe* (pp. 49–54). Nuremburg, Germany.

Ellis, G., & Lorenz, R. D. (1999). Comparison of motion control loops for industrial applications. In *Proceedings of IEEE industry applications society annual meeting* (pp. 2599–2605). Phoenix, AZ.

Haddad, W. M., & Chellaboina, V. (2008). *Nonlinear dynamical systems and control*. New Jersey: Princeton University Press.

Li, S., & Liu, Z. (2009). Adaptive speed control for permanent-magnet synchronous motor system with variations of load inertia. *IEEE Transactions on Industrial Electronics*, *56*(8), 3050–3059.

Liu, Y., & Li, T. (2008). Design and implementation of an ASIC-based four-axis position servo system. In *Proceedings of the electrical machines and systems international conference* (pp. 3697–3701). Wuhan, China.

Mohamed, Y. A. (2007). Design and implementation of a robust current control scheme for a PMSM vector drive with a simple adaptive disturbance observer. *IEEE Transactions on Industrial Electronics*, *54*(4), 1981–1988.

Ohm, D. Y. (1994). Analysis of PID and PDF compensators for motion control systems. In *Proceedings of IEEE IAS annual meeting* (pp. 1923–1929). Denver, CO.

Pajchrowski, T., & Zawirski, K. (2008). Application of fuzzy logic techniques to robust speed control of PMSM. In *Proceedings of 13th power electronics and motion control conference* (pp. 1198–1203). Poznan, Poland.

Perdikaris, G. A. (1999). Microcomputer control of a motor drive system. In *Proceedings of IEEE industry applications society annual meeting* (pp. 1056–1060). Phoenix, AZ.

Romeral, L., & Chekkouri, M. R. (2002). Fuzzy adaptive PDF controller for motion control systems. In *Proceedings of the IEEE international symposium on industrial electronics* (pp. 299–304). L'Aquila, Italy.

Shen, B. H., & Tsai, M. C. (2006). Robust dynamic stiffness design of linear servo motor drives. *Control Engineering Practice*, *14*(11), 1325–1336.

Tsai, M. C., & Shen, B. H. (2007). Synchronization control of parallel dual inverted pendulums driven by linear servomotors. *IET Control Theory & Applications*, *1*(1), 320–327.

Wallace, I. T., Novotny, D. W., Lorenz, R. D., & Divan, D. M. (1994). Increasing the dynamic torque per ampere capability of induction machines. *IEEE Transactions on Industry Applications*, *30*(1), 146–153.